JOURNAL OF SOLID STATE CHEMISTRY 30, 345–352 (1979)

The Preparation and Crystal Structures of $BiReO_4$ and $BiRe_2O_6$

A. R. RAE SMITH AND A. K. CHEETHAM*

Department of Chemical Crystallography, 9, Parks Road, Oxford, OX1 3PD, England

Received September 18, 1978; in revised form February 12, 1979

The crystal structures of two new oxides, $BiReO_4$ and $BiRe_2O_6$, have been determined by single-crystal X-ray methods using an Enraf–Nonius CAD-4F diffractometer. $BiReO_4$ crystallizes as red metallic needles in the space group *Cmcm*, cell dimensions $a = 3.839(1)$ Å, $b = 14.914(2)$ Å, $c = 5.534(1)$ Å, $Z = 4$. The structure consists of sheets of corner-shared octahedra (composition ReO_4) linked by Bi atoms ($R = 2.55\%$). $BiRe_2O_6$ crystallizes as black metallic plates in the space group $C2/m$, cell dimensions $a = 5.516(1)$ Å, $b = 4.906(1)$ Å, $c = 8.384(1)$ Å, $\beta = 106.71(1)°$, $Z = 2$. The structure consists of layers containing Re_2O_{10} units linked together by corner sharing of the octahedra, alternating with layers of Bi atoms ($R = 2.61\%$). The structure is disordered due to the random stacking of the Re layers. The Re–Re distance of 2.5 Å in the Re_2O_{10} unit is comparable to that found in similar compounds. Both compounds exhibit stereochemically active lone pairs.

Introduction

Crystals of the two title compounds were prepared and their crystal structures determined during an investigation of the system Bi–Re–O. The system was chosen in view of the large number of compounds which have been found in the La–Re–O system (*1*), and also because of possible catalytic activity similar to that found in bismuth molybdenum oxides (*2*).

Experimental

Preparation

The crystals were formed by vapor transport along a temperature gradient. Mixtures of the constituent oxides (ReO_3 and Bi_2O_3) were ground together in an agate mortar and 30 mg of the mixture were placed in a silica tube 7 cm long, 1 cm diameter, which was sealed off under vacuum. The tubes were placed centrally and lengthwise in a muffle furnace 60 cm in length at temperatures between 600 and 800°C. Crystals of up to 0.5 mm in size form within a few hours.

The major products of reaction when the ratio $Bi_2O_3 : ReO_3$ is between 1 and 2 are Bi_3ReO_8 and $BiRe_2O_6$. The vapor species appear to be Bi atoms and Re_2O_7. ReO_3 disproportionates above 400°C into ReO_2 and Re_2O_7, so presumably Bi_2O_3 oxidizes ReO_2 to Re_2O_7. Guinier photographs taken at intermediate stages of the reaction confirm the presence of ReO_2, Bi, Bi_3ReO_8, and $BiRe_2O_6$. Reaction takes place at the cool end of the tube to form colorless crystals of Bi_3ReO_8 intermingled with black plates of $BiRe_2O_6$. The compound Bi_3ReO_8 appears to be one of the most stable compounds in the system and its fluorite-related crystal structure is presently under investigation.

In one preparation at the lower temperature of 550°C, a small number of red metallic

* To whom correspondence should be addressed.

0022–4596/79/120345–08$02.00/0

needles resembling ReO_3 in appearance were formed. These proved after analysis to have the composition $BiReO_4$.

The relative proportions of the starting materials do not appear to be critical, nor does the initial oxidation state of rhenium: Thus, reaction between Bi_2O_3 and Re metal yields the same two major products (Bi_3ReO_8 and $BiRe_2O_6$) but with a higher proportion of Bi metal left after reaction. However, while it is possible to prepare $BiRe_2O_6$ in bulk by reaction of appropriate amounts of bismuth and rhenium metal oxides (for example, $Bi+2ReO_3$), $BiReO_4$ has so far only appeared as a by-product.

Chemical Analysis

Analysis for the metal atom ratio was carried out on a JEOL 100CX-TEMSCAN analytical electron microscope with a KEVEX Li drifted silicon energy dispersive X-ray detector.

For thin crystals the effects of absorption and fluorescence encountered with bulk specimens are negligible and the relative concentrations are related to the X-ray emission intensities by the simple equation $x_1/x_2 = k(I_1/I_2)$, where x_1, x_2, I_1, and I_2 represent, respectively, the concentrations and X-ray emission intensities of the two species (*3*).

Phases were identified by selected area diffraction: This technique was also used to indicate that crystals were suitably thin for analysis. An estimate of the absorption and other interference taking place was afforded by the ratios of the intensities of the Re $M\alpha/L\alpha$ and Bi $M\alpha/L\alpha$ lines. These ratios decrease rapidly as the thickness increases since the low-energy X rays are more heavily affected by absorption. Thus for rhenium the absorption coefficients are $\mu_{BiM\alpha} = 2853.5$, $\mu_{BiL\alpha} = 208.8$, $\mu_{ReM\alpha} = 0.0$, and $\mu_{ReL\alpha} = 145.8\ cm^{-1}$, and for bismuth they are $\mu_{BiM\alpha} = 0.0$, $\mu_{BiL\alpha} = 113.4$, $\mu_{ReM\alpha} = 1728.1$, and $\mu_{ReL\alpha} = 203.7\ cm^{-1}$ (*4*).

The factor k in the above equation was obtained from analysis of crystals of Bi_3ReO_8 (this compound had been independently analyzed by bulk X-ray fluorescence) and is fortuitously about 1. The thickness of the crystals used for analysis was less than 0.5 μm and the operating voltage of the microscope was 40 kV.

The spectra are shown in Fig. 1 and the results of the analyses indicated that the two phases of interest had Bi:Re ratios of 1:1 and 1:2, respectively. Analysis for the total oxidation state was not possible owing to the small amount of sample; however, from considerations of the crystallographic symmetry and cell volume, the formulas assigned

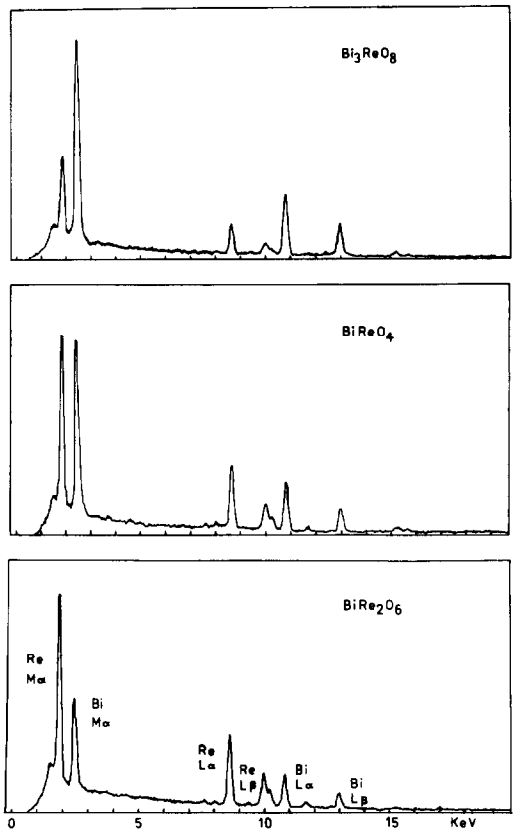

FIG. 1. X-Ray emission spectra of Bi_3ReO_8, $BiReO_4$, and $BiRe_2O_6$. Counting time 60 sec. Average counting rate (after processing) 2000 counts sec^{-1}.

seemed reasonable and were indeed confirmed by the structure solution.

Data Collection

X-Ray single-crystal data collection was carried out on a PDP-8 controlled Enraf–Nonius CAD4F diffractometer using Mo$K\alpha$ radiation. Accurate orientation matrices and cell dimensions were obtained by automatic centering of 25 strong reflections with $18 < \theta < 25°$. Intensities were collected using a θ–2θ scan width of $1 + 0.35 \tan\theta$ degrees. Intensity control was carried out on three intense reflections every 1.5 hr and the orientation was checked after every 200 reflections. For the analytical absorption correction, the crystals were set up on an optical goniometer to identify and measure the principal faces.

Structure Refinement[1]

$BiReO_4$

Preliminary Weissenberg photographs indicated orthorhombic symmetry with systematic absences hkl, $h+k=2n$, $h0l$, $l=2n$, reducing the possible space groups to $Cmcm$, $Cmc2_1$, and $C2cm$ ($=Ama2$). Final cell dimensions obtained were $a = 3.839(1)$, $b = 14.914(2)$, and $c = 5.534(1)$ Å. Intensities of 1897 reflections were collected in the NEEDLE[2] mode on a crystal with approximate dimensions $0.23 \times 0.05 \times 0.05$ mm over the range $0 < \theta < 45°$. Azimuthal (Ψ) scans were then collected for 16 independent reflections distributed over the whole reflection sphere. Lorentz and polarization corrections were applied, followed by an analytical absorption correction ($\mu = 931$ cm^{-1}) described by Templeton (*5*). The application of the absorption correction reduced the maximum peak to trough ratio in the Ψ scans from 5.54 to 1.22. Equivalent reflections were then merged to give 685 reflections with $I/\sigma(I) > 3$ (merging R factor 4%).

The metal atom positions were deduced from the Patterson function and two cycles of refinement reduced the R factor (weighted R factor) to 9.45(11.50)%. A difference Fourier revealed the position of the oxygen atoms and enabled the metal atom sites to be assigned. A further two cycles of refinement of all parameters, allowing the metal atoms to vibrate anisotropically, reduced the R factor to 7.27(9.17)%. A correction for secondary extinction (*6*) was then made, requiring a further four cycles of refinement to give a final R factor of 2.55(3.31)%. A subsequent difference Fourier revealed no peaks larger than $2e$ Å^{-3}. The structural data are shown in Table 1.

$BiRe_2O_6$

Care was necessary in the preparation of the crystals due to the ease of twinning across the ab plane (b^*c^* net). The crystals grow either as plates perpendicular to the c axis or as thick needles along the ⟨110⟩ directions.

Preliminary Weissenberg photographs indicated monoclinic symmetry with systematic absences hkl, $h+k=2n$, giving the possible space groups $C2/m$, $C2$, and Cm. Final cell dimensions obtained were $a = 5.516(1)$ Å, $b = 4.906(1)$ Å, $c = 8.384(1)$ Å, $\beta = 106.71(1)°$. Intensities of 958 reflections were collected in the FLAT[2] mode on a crystal with approximate dimensions $0.1 \times 0.1 \times 0.02$ mm over the range $0 < \theta < 35°$. Ψ scans were collected for three reflections with $\chi \approx 90°$. Lorentz and polarization corrections were applied, followed by an analytical absorption correction (*5*)

[1] All calculations for both structures were performed using the Oxford CRYSTALS package on an ICL 1906A computer. Values for scattering factors and anomalous dispersion coefficients were taken from Vol. IV of the International Tables for X-Ray Crystallography. Structure factor tables have been deposited with the National Auxiliary Publications Service.

[2] In the NEEDLE and FLAT modes, the controlling program calculates the position of minimum absorption for each reflection from the input vector (representing the needle axis or the vector perpendicular to the plate) and rotates the crystal about the scattering vector to reach the nearest position to the optimum.

TABLE I

STRUCTURAL PARAMETERS FOR $BiReO_4$[a]

Atom	Position	x/a	y/b	z/c	U_{11}	U_{22}	U_{33}
Re	$c(4)$	0.0	0.0839(1)	0.25	0.0038(2)	0.0043(2)	0.0028(2)
Bi	$c(4)$	0.0	0.3120(1)	0.25	0.0083(2)	0.0068(2)	0.0071(2)
O(1)	$a(4)$	0.0	0.0	0.0	U[iso] = 0.008(1)		
O(2)	$c(4)$	0.0	0.591(1)	0.25	U[iso] = 0.008(1)		
O(3)	$f(8)$	0.0	0.188(1)	0.485(1)	U[iso] = 0.007(1)		

Selected distances and angles

Distances (Å)	
Re–O(1) [×2] 1.87(1)	Bi–O(3) [×2] 2.26(1)
Re–O(2) [×2] 1.92(1)	Bi–O(3) [×4] 2.42(1)
Re–O(3) [×2] 2.02(1)	Closest O–O distance 2.60(1)
Angles (°)	
O(1)–Re–O(1) 95.8(1)	O(3)–Bi–O(3) 69.7(1)
O(1)–Re–O(2) 92.2(1)	O(3)–Bi–O(3) 70.0(2)
O(1)–Re–O(3) 92.2(1)	O(3)–Bi–O(3) 74.9(2)
O(1)–Re–O(3) 172.1(1)	O(3)–Bi–O(3) 105.1(2)
O(2)–Re–O(2) 173.6(4)	O(3)–Bi–O(3) 110.5(1)
O(2)–Re–O(3) 87.5(2)	O(3)–Bi–O(3) 179.8(2)
O(3)–Re–O(3) 79.9(3)	

[a] ESDs in parentheses; space group *Cmcm* (No. 63).

($\mu = 968\ cm^{-1}$). The application of the absorption correction reduced the maximum peak to trough ratio in the Ψ scans from 10.0 to 1.3. Equivalent reflections were then merged to give 492 reflections with $I/\sigma(I) > 3$ (merging R factor 3.6%).

The metal atom positions were deduced from the Patterson function and two cycles of refinement reduced the R factor to 9.40(10.98)%. A difference Fourier revealed the positions of the oxygen atoms, and a further three cycles of refinement of all parameters gave an R factor of 4.92(6.29)%. A correction for secondary extinction (*6*) was then made, giving a final R factor of 2.61(3.53)%. A subsequent difference Fourier revealed no peaks larger than $2e\ Å^{-3}$. The structural data are shown in Table II.

Discussion

$BiReO_4$

Very few oxides containing rhenium in a formal oxidation state of V have been prepared except for a number of perovskites A_2M(III)ReO_6 (*7*), some compounds $M_2Re_2O_7$ possessing the pyrochlore structure (*8*), and the compounds $Ln_4Re_2O_{11}$ (*9*). Re_2O_5 itself is very unstable with respect to disproportionation and has only recently been characterized (*10*).

The structure of $BiReO_4$ is closely related to that of α-$BiNbO_4$ (*11*) and $BaMnF_4$ (*12*), consisting of sheets of corner-sharing ReO_6 octahedra perpendicular to the b axis linked by Bi atoms (alternate sheets being displaced by one-half octahedron). The relationship between the structures is similar to that between ReO_3 and WO_3 (and other tilted perovskite structures). Thus although the rhenium atoms are slightly displaced from the centers of the octahedra, the octahedra are not tilted as in ferroelastic $BiNbO_4$ or rotated as in $BaMnF_4$.

Continuing the analogy, one would expect $BiReO_4$ (containing Re(V) with a d^2 configuration) to be metallic. In appearance it is similar to ReO_3 (d^1), and although no single crystals were large enough for stan-

TABLE II

STRUCTURAL PARAMETERS FOR $BiRe_2O_6$[a]

Atom	Position	x/a	y/b	z/c	U_{11}	U_{22}	U_{33}	U_{13}
Re	$i(4)$	0.0439(1)	0.0	0.3613(1)	0.0023(3)	0.0078(3)	0.0027(3)	0.0008(1)
Bi[b]	$g(4)$	0.0	0.520(3)	0.0	0.0067(3)	0.0097(34)	0.0066(3)	0.0014(2)
O(1)[b]	$j(8)$	0.402(2)	0.344(3)	0.138(2)		U[iso] = 0.007(2)		
O(2)[b]	$j(8)$	0.298(2)	0.277(3)	0.433(2)		U[iso] = 0.008(2)		
O(3)[b]	$j(8)$	0.282(2)	0.782(3)	0.277(2)		U[iso] = 0.008(2)		

Selected distances and angles

Distances (Å)

Re–Re	2.508(1)	Bi–O(1)	2.35(1)
Re–O(1)	1.97(1)		2.29(1)
Re–O(2)	1.92(1)		2.12(2)
	1.97(1)		2.28(2)
	2.02(1)	Bi–O(3)	2.82(2)
Re–O(3)	1.98(1)		2.72(2)
	1.98(1)	Closest O–O distance	2.60(2)

Angles (°)[c]

O(1)–Re–O(2)	94.3(6)	O(2)–Re–O(2)	102.1(5)
O(1)–Re–O(2)	87.2(6)	O(2)–Re–O(3)	90.0(5)
O(1)–Re–O(2)	169.2(6)	O(2)–Re–O(3)	81.1(6)
O(1)–Re–O(3)	89.6(6)	O(2)–Re–O(3)	176.8(6)
O(1)–Re–O(3)	83.3(6)	O(3)–Re–O(3)	89.2(3)
O(2)–Re–O(2)	91.0(3)	Re–O(2)–Re	90.9(4)

(a)		(b)	
O(1A)–Bi–O(1B)	77.8(4)	O(1A)–Bi–O(1B)	77.8(4)
O(1B)–Bi–O(1D)	101.1(4)	O(1A)–Bi–O(1D)	68.5(6)
O(1D)–Bi–O(1C)	82.4(5)	O(1D)–Bi–O(1C)	77.8(4)
O(1C)–Bi–O(1A)	98.6(4)	O(1C)–Bi–O(1B)	68.5(6)
O(1B)–Bi–O(1C)	175.3(6)	O(1B)–Bi–O(1D)	136.7(9)
O(1A)–Bi–O(1D)	176.7(4)	O(1A)–Bi–O(1C)	76.6(8)
O(3A)–Bi–O(1A)	95.6(5)	O(3A)–Bi-O(1A)	95.6(5)
O(3A)–Bi–O(1B)	61.8(4)	O(3A)–Bi–O(1B)	61.8(4)
O(3A)–Bi–O(1C)	121.9(6)	O(3A)–Bi–O(1C)	130.1(5)
O(3A)–Bi–O(1D)	86.6(6)	O(3A)–Bi–O(1D)	145.2(5)
O(3A)–Bi–O(3B)	176.4(5)	O(3A)–Bi–O(3B)	123.6(8)

[a] ESDs in parentheses; space group $C2/m$ (No. 12).
[b] Total occupancy of these sites is half the full multiplicity.
[c] For labeling of atoms see Fig. 4.

dard conductivity measurements, a simple two-probe experiment indicated that the resistance perpendicular to the ReO_4 sheets was much higher than that parallel to the sheets.

Another compound which adopts a related structure is Sb_2O_4. This compound was used to illustrate the stereochemical activity of the lone pair of the M(III) atom by Galy *et al.* (*13*). They pointed out that the anomalously large volume per anion in the unit cell could be explained by assigning the lone pair to an anion site. The combination of anions and lone pairs then forms a close-packed arrangement with a volume of around 16 Å^3 per anion. In $BiReO_4$, the tunnels formed by the vacant anion sites are clearly visible (Fig. 2) and the irregular coordination of the Bi

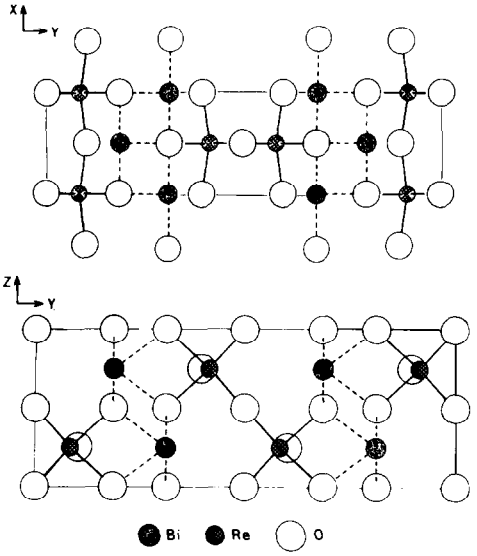

FIG. 2. Projections of $BiReO_4$ down the c and a axes. Full lines represent Re–O close contacts, broken lines Bi–O close contacts. The unit cell is outlined.

atom (six oxygen atoms at the corners of a cube with one edge missing) again suggests a stereochemically active lone pair.

$BiRe_2O_6$

Oxides containing Re in two formal oxidation states but on the same crystallographic site are found in the La–Re–O system, e.g., $La_4Re_6O_{19}$ (*14*). The same situation is found in $BiRe_2O_6$.

The crystal structure of $BiRe_2O_6$ consists of slabs of octahedrally coordinated Re separated by a layer of Bi atoms. Within the Re layers, pairs of edge-sharing octahedra form Re_2O_{10} units which are themselves linked to other such units by corner sharing (Fig. 3). This method of coordination is found in a number of mixed metal oxides, for example, $La_4Re_6O_{19}$ (*14*) and $Bi_3Ru_3O_{11}$ (*15*). The parent structure of these compounds is $KSbO_3$ (*16*), where the Sb_2O_{10} units form a three-dimensional framework with the other atoms filling the large interstices.

The stacking of the Re layers in $BiRe_2O_6$ is disordered. The oxygen atoms are split into two sets by the symmetry operators x, y, z; $-x, -y, -z$; $\frac{1}{2}+x, \frac{1}{2}-y, z$; and $\frac{1}{2}-x, \frac{1}{2}+y, -z$ to obtain octahedral coordination about the rhenium atom. It is possible to obtain an ordered arrangement of oxygen atoms in the noncentrosymmetric space groups *Cm* and *C*2, but these give rise to unlikely coordination geometries around rhenium. *Cm* gives a trigonal prismatic coordination while *C*2 leaves half the Re atoms uncoordinated.

The difference between the two sets of oxygen atoms can be approximated by a shift of 1 Å along the c axis and, in view of the open coordination about the Bi atom (Figs. 3 and 4), it is not difficult to see how this

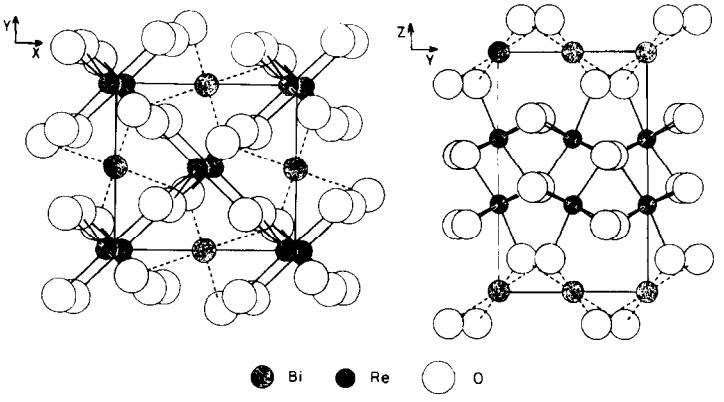

FIG. 3. Projections of $BiRe_2O_6$ down the c and a axes. Full lines represent Re–O close contacts, broken lines Bi–O close contacts. The unit cell is outlined.

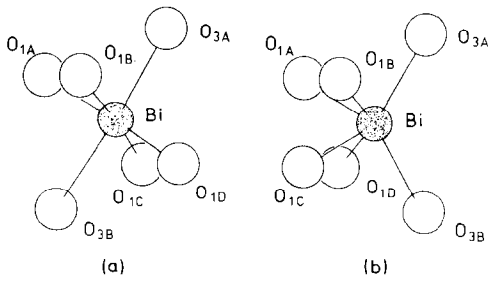

FIG. 4. Coordination of Bi in $BiRe_2O_6$ projected down the *a* axis (a) if adjacent Re layers contain same set of oxygen atoms, and (b) if adjacent Re layers contain different set of oxygen atoms.

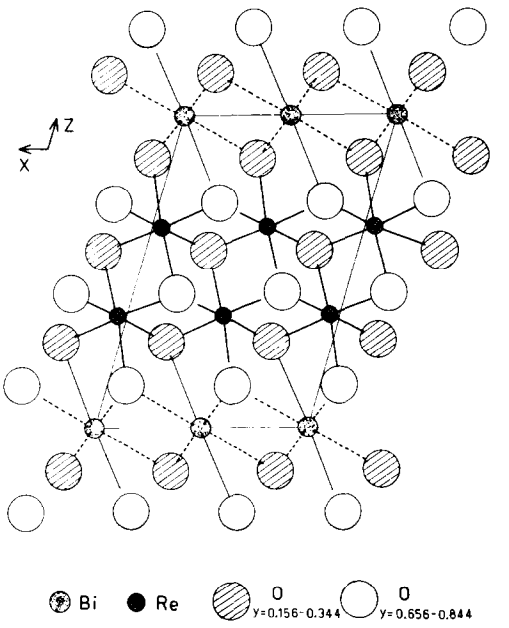

FIG. 5. Projection of $BiRe_2O_6$ down the *b* axis. The unit cell is outlined. At the top boundary, adjacent Re layers contain different sets of oxygen atoms, while at the bottom boundary, adjacent layers contain the same set.

disorder might occur. Support for the disordered model is given by the high anisotropic temperature factor ($U_{22} = 0.018$) obtained for Bi during early refinements. This was replaced in subsequent refinements by a static displacement of Bi from the special position 0, $\frac{1}{2}$, 0. Although Guinier photographs showed no evidence for any doubling of the cell, some Weissenberg photographs taken on crystals from a later preparation showed a weak intensity for the primitive reflections.

The short Re–Re distance of 2.5 Å perpendicular to the sheets indicates a metal–metal bond of the same order as that found in ReO_2 and $La_4Re_6O_{19}$ (*17*), suggesting delocalization of the remaining $\frac{3}{2}d$ electrons per Re atom. A simple two-probe experiment showed that the crystals were of low resistance.

As in $BiReO_4$, the cell volume (volume per anion $BiRe_2O_6 = 18$ Å^3, volume per anion $BiRe_2O_6E = 15.4$ Å^3)[3] and the relatively open coordination about the Bi atom indicate that the lone pair is exerting some stereochemical effect. The tunnels parallel to the *a* axis are visible in Fig. 3, and the vacancies in the anion lattice can be seen in Fig. 5. Figure 5 shows two boundaries of the unit cell. At the bottom of the figure, adjacent Re layers contain the same set of oxygen atoms, while at the top boundary they contain different sets. The vacancies are particularly evident at the top boundary. Thus the shaded oxygen atoms form a continuous layer in the hexagonal close-packed lattice, while the unshaded oxygen atoms have a line of vacancies above the bismuth atoms.

There does not appear to be any other compound which adopts the $BiRe_2O_6$ structure. The closest analogous structure is $PbSb_2O_6$ (*18*), which also consists of alternating layers of octahedrally coordinated Sb and Pb atoms in a hexagonal close-packed oxygen lattice. However, the layers lie in a different direction with respect to the oxygen lattice, and contain chains of edge-sharing SbO_6 octahedra rather than discrete Sb_2O_{10} units. Moreover, in $BiRe_2O_6$, the coordination of the Bi atoms is far from octahedral (see Fig. 4), with four oxygen atoms at about 2.3 Å and two additional atoms at 2.75 Å.

[3] Using the nomenclature of Ref. (*13*).

Acknowledgments

We wish to thank the Science Research Council for a grant (GR/A/3320) toward the purchase of an electron microscope and for the provision of a studentship for one of us (A.R.R.S.). We are also grateful to Hermann Starck Berlin for the provision of rhenium.

References

1. G. BAUD AND M. CAPESTAN, *Bull. Soc. Chim. Fr.*, 4685 (1967), 3999 (1969); O. MULLER AND R. ROY, *Mater. Res. Bull.* **4**, 349 (1969).
2. G. C. A. SCHUIT, *J. Less Common Metals* **36**, 329 (1974).
3. S. J. B. REED, "Electron Microprobe Analysis," p. 326, Cambridge Univ. Press, London/New York (1975).
4. K. F. J. HEINRICH, in "The Electron Microprobe" (T. D. McKinley, K. F. J. Heinrich, and D. B. Wittry, Eds.), p. 350, Wiley, New York (1966).
5. L. K. TEMPLETON AND D. H. TEMPLETON, *in* "Abstracts, Summer Meeting of the American Crystallographic Association, Storrs, Conn.," p. 143 (1973).
6. A. C. LARSON. *in* "Crystallographic Computing" (F. R. Ahmed, Ed.), p. 291, Munksgaard, Copenhagen (1970).
7. A. W. SLEIGHT, J. LONGO, AND R. WARD, *Inorg. Chem.* **1**, 245 (1962).
8. P. C. DONOHUE, J. M. LONGO, R. D. ROSENSTEIN, AND L. KATZ, *Inorg. Chem.* **4**, 1152 (1965); R. SCHOLDER AND P. P. PFEIFFER, *Angew. Chem. Int. Ed. Engl.*, **2**, 265 (1963).
9. K. A. WILHELMI, E. LAGERVALL, AND O. MULLER, *Acta. Chem. Scand.* **24**, 3406 (1970).
10. D. COLAITIS, D. LEBAS, AND C. LECAILLE, *Mater. Res. Bull.* **8**, 627 (1973).
11. E. T. KEVE AND A. C. SKAPSKI, *J. Solid State Chem.* **8**, 159 (1973).
12. E. T. KEVE, S. C. ABRAHAMS, AND J. L. BERNSTEIN, *J. Chem. Phys.* **51**, 4928 (1969).
13. J. GALY, G. MEUNIER, S. ANDERSSON, AND A. ÅSTRÖM, *J. Solid State Chem.* **13**, 142 (1975).
14. N. MORROW AND L. KATZ, *Acta Crystallogr. Sect. B* **24**, 1466 (1968); J. M. LONGO AND A. W. SLEIGHT, *Inorg. Chem.* **7**, 108 (1968).
15. F. ABRAHAM AND D. THOMAS, *Bull. Soc. Fr. Mineral. Crystallogr.* **98**, 25 (1975).
16. P. SPIEGELBERG, *Ark. Kemi Mineral. Geol.* **14A**, No. 5 (1940).
17. T. P. SLEIGHT, C. R. HARE AND A. W. SLEIGHT, *Mater. Res. Bull.* **3**, 437 (1968).
18. A. MAGNÉLI, *Ark. Kemi Mineral. Geol.* **15B**, No. 3 (1941).